Journal of Controlled Release 276 (2018) 140–149

Contents lists available at ScienceDirect

Journal of Controlled Release

journal homepage: www.elsevier.com/locate/jconrel

Readily prepared biodegradable nanoparticles to formulate poorly water soluble drugs improving their pharmacological properties: The example of trabectedin

Umberto Capasso Palmiero[a], Lavinia Morosi[b], Ezia Bello[b], Marianna Ponzo[b], Roberta Frapolli[b], Cristina Matteo[b], Mariella Ferrari[b], Massimo Zucchetti[b], Lucia Minoli[c,d], Marcella De Maglie[c], Pierpaolo Romanelli[c], Massimo Morbidelli[e], Maurizio D'Incalci[b,1], Davide Moscatelli[a,*,1]

[a] Department of Chemistry, Materials and Chemical Engineering "Giulio Natta", Politecnico di Milano, Via Mancinelli 7, 20131 Milano, Italy
[b] Department of Oncology, IRCCS, Istituto di Ricerche Farmacologiche Mario Negri, Via La Masa 19, 20156 Milano, Italy
[c] Mouse & Animal Pathology Laboratory, Fondazione Filarete, Viale Ortles, 22/4, 20139 Milano, Italy
[d] Department of Veterinary Medicine, Università degli Studi di Milano, via Celoria 10, 20133 Milano, Italy
[e] Department of Chemistry and Applied Biosciences, Institute for Chemical and Bioengineering, ETH Zurich, Switzerland

ARTICLE INFO

Keywords:
Nanoparticles
Polycaprolactone
Biodegradable
Polyethylen glycol
Trabectedin
Phlebitis
Vascular toxicity

ABSTRACT

The improvement of the pharmacological profile of lipophilic drug formulations is one of the main successes achieved using nanoparticles (NPs) in medicine. However, the complex synthesis procedure and numerous post-processing steps hamper the cost-effective use of these formulations. In this work, an approach which requires only a syringe to produce self-assembling biodegradable and biocompatible poly(caprolactone)-based NPs is developed. The effective synthesis of monodisperse NPs has been made possible by the optimization of the block-copolymer synthesized via a combination of ring opening polymerization and reversible addition-fragmentation chain transfer polymerization. These NPs can be used to formulate lipophilic drugs that are barely soluble in water, such as trabectedin, a potent anticancer therapeutic. Its biodistribution and antitumor activity have been compared with the commercially available formulation Yondelis®. The results indicate that this trabectedin NP formulation performs with the same antitumor activity as Yondelis®, but does not have the drawback of severe local vascular toxicity in the injection site.

1. Introduction

Polyester-based nanoparticles (NPs) have gained attention in the last decades as biodegradable delivery systems for lipophilic therapeutics in the treatment of a large variety of diseases, e.g. cancer [1,2]. In the treatment of solid tumors, the improvement in the therapeutic index of the drug is achieved by the enhanced permeability and retention (EPR) effect [3]. The leaky vasculature of the tumor blood vessels allows for the passage of macromolecules bigger than 40,000 g/mol, while the impaired lymphatic drainage leads to their retention in the extracellular environment. However, the progress of the nanotechnology has been hampered by the heterogeneity of the solid tumors in the patients [4]. In fact, the pore of the vessel tissues differs both within the same and different types of tumors. In addition, several portions of the tumor tissue may experience hypoxia and completely absence of vasculature or compressed blood vessels, making it impossible to take advantage of the EPR effect. The accumulation of the NPs developed so far in solid tumors is still limited to a median of 0.7% of the administered dose [5]. Target agents are often added to increase the selectivity of the NPs, but the improvement is only minimal. For this reason, several nano-based therapeutics approved by the Food and Drug Administration (FDA), such as Doxil®, have resulted in only a marginal improvement in the overall survival of the patients [6]. The most important results in the NP-based therapeutics approved so far rely on the reduction of the overall toxicity of the formulation by removing toxic excipients and/or solvents that are used to improve their solubility and by reducing the drug related side effects. An example is the paclitaxel (PTX) where the toxic cremophor EL of the Taxol® has been removed in the Abraxane® and Genexol® new formulations [7,8]. However, the complexity related to the NP manufacturing process can lead to an increase in the final cost of these "re-formulations" [9] and problems in batch to batch reproducibility, significantly reducing the availability of

* Corresponding author.
E-mail address: davide.moscatelli@polimi.it (D. Moscatelli).
[1] Maurizio D'Incalci and Davide Moscatelli co-last authors.

https://doi.org/10.1016/j.jconrel.2018.03.005
Received 14 December 2017; Received in revised form 2 March 2018; Accepted 4 March 2018
Available online 07 March 2018
0168-3659/

these treatments among the patient population. For example, the manufacturing difficulties in the synthesis of Doxil® have led to a drug shortage in the market that the approval of nano-generics have only partially solved [10]. In fact, even in the production of an analogous NP formulation, the same level of quality controls, high-trained specialists and good manufacturing practices (GMPs) are necessary to assure pharmaceutical, clinical and physical equivalence of these nanotherapeutics. These technical issues often dissuade pharmaceutical companies from entering the nanotechnological field [11,12]. For this reason, a proper balance between simplicity and complexity of the drug delivery systems must be taken into account from the very first step of the NP design and development [10]. This is particularly true in the case of polyester based-NPs, which are one of the most diffused class of nanotherapeutics studied in literature due to their biodegradability and biocompatibility [13], but that have resulted in only few products being investigated in clinical trials [11] and entering into the market. They are preferentially synthesized via nanoprecipitation [14] where amphiphilic copolymer and a drug are dissolved in a water-miscible organic solvent that is, in turn, added dropwise to an aqueous solution. The rapid diffusion of the solvent in the bulk phase under turbulent conditions generates polymer NPs able to encapsulate a lipophilic therapeutic in a "one-step" procedure with a relatively high encapsulation efficiency. However, this method presents negative aspects, such as (i) the need of using high amount of organic solvent and sometimes toxic surfactants, (ii) the poor control over the NP size and size distribution, and (iii) the reproducibility issues. In particular, the turbulent conditions in the mixing step have a significant impact on the NP quality [15] and, for this reason, several devices have been developed to improve the contact efficiency between the aqueous and organic phase. These devices are generally micro-channels in which the organic and the aqueous phases are fed in a countercurrent and intimately mixed under turbulent conditions; one example is the T-mixer [16]. In order to eliminate the large amount of organic solvent and the unloaded drug in the system after the drug-loaded NPs are obtained, dialysis must be performed to prevent undesired effects from the cytotoxicity of the solvent and uncontrollable release of the drug. Moreover, after this step, an appropriate storage of the final product is needed. Even though a colloidal suspension is generally stable, some agglomeration can occur, especially when the time between drug loading and administration of the drug-loaded NPs is too long [13]. In addition, water must be removed to avoid NP degradation from hydrolysis of the ester bond, which would compromise the physicochemical stability of the colloids. Among the various methods to increase the stability of the NPs, one of the most commonly used is lyophilization [17]. After complete desiccation, NPs are obtained in the form of a dry powder that is easily handled and stored; in most cases the freeze-dried particles are readily dispersible in aqueous solutions. It is also true, however, that freezing is the most aggressive step of the freeze-drying operation; in order to improve the resistance of the NPs and avoid alteration of the suspension, the addition of a cryoprotectant is required [18]. Consequently, there is a clear need to develop a simpler and reliable method to produce NPs that avoids the use of sophisticated devices and the above mentioned post-production methods, such as dialysis and lyophilization. It is noteworthy to mention that all the above reported post-processing steps are required for the large majority of the nanotherapeutics developed so far, independently from their nature and composition [10], leading to the establishment of complex quality control systems and difficulties in the application of GMPs.

In this work, a library of amphiphilic biodegradable block-copolymers has been developed to formulate lipophilic drugs into NPs directly at the bed of the patient via a simplified nanoprecipitation method that requires only a syringe and a small amount of an organic solvent (i.e. DMSO). This has been possible via the fine-tuning of the hydrophilic/lipophilic balance (HLB) of these self-assembling "comb-like" materials and the optimization of the various components of the final formulation: the drug, the organic solvent, the aqueous medium, and the polymeric surfactant. In particular, the combination of reversible addition-fragmentation chain transfer (RAFT) polymerization and the ring opening polymerization (ROP) have allowed for an additional degree of freedom in the common linear polyester-polyethylen glycol (PEG) block-copolymers [19], which could pave the way to greater control over their structure and molecular weight. The impact of turbulent conditions on the NP formation has been studied by comparing the quality of the NPs obtained via the syringe method and the ones produced via a set-up already reported in literature that uses a mixing device [16]. Then this method has been used to load trabectedin (ET-743) into NPs without the need of any purification steps in order to provide a formulation that can be easily produced by the end-user from the native block-copolymer.

ET-743 is marine alkaloid first isolated from the Caribbean *Ecteinascidia turbinate* that has been developed in the clinic because of its striking antitumor activity in several preclinical models and its unique mechanism of action [20–22]. It binds to the N2 position of guanines in the minor groove of DNA and affects transcription in a gene and promoter-specific fashion [23]. The drug causes cancer cell death and modifies the tumor microenvironment by reducing the number of tumor associated macrophages and inhibiting the production of inflammatory and angiogenic factors [24,25]. It is approved in Europe for the second line therapy of soft tissue sarcoma and in combination with pegylated liposomal doxorubicin in ovarian cancer patients, and in US for the second line therapy of leiomyosarcomas and liposarcomas. ET-743 cannot be injected in a peripheral vein because it causes severe local toxicity with painful erythema along the blood vessel and sclerotic phlebitis at the site of injection. It therefore requires administration through a central venous catheter [26], a procedure associated with increased health care costs, morbidity and possible serious medical complications, e.g. bloodstream infections. For this reason, ET-743 has been chosen as candidate for this technological platform. The NP-based formulation contains < 1.5 vol.% of DMSO and presents the same antitumor activity as the currently approved clinical formulation (Yondelis®), but with a better toxicological profile. In particular, it shows the ability to prevent local toxicity, leaving no sign of phlebitis at the site of the injection and allowing for a classic i.v. administration of the drug compared to the ones currently based on venous catheters. This formulation is expected to reduce the ET-743 related side effects and to significantly improve patient compliance to the treatment.

2. Materials and methods

2.1. Materials

ε-caprolactone (CL, 97%), 2-hydroxyethyl methacrylate (HEMA, 97%), stannous octoate [$Sn(Oct)_2$, 98%], Sodium sulfate (Na_2SO_4, 99%), poly(ethylene glycol) methyl ether methacrylate ($PEG_{45}MA$, Mn 2000 g/mol, 80 wt.% in water), 4,40-azobis(4-cyanovaleric acid) (ACVA, 98%), 4-cyano-4-(phenylcarbonothioylthio)-pentanoic acid (CPA, > 97%), ethanol (EtOH, 99,8%), dimethyl sulfoxide (DMSO), tetrahydrofuran (THF, ≥99.9%), chloroform-*d* were purchased from Sigma-Aldrich (St. Louis, Missouri, United States) and used without further treatment except when specifically noted. All the solvents used were of analytical-grade purity and were purchased from Sigma-Aldrich. $PEG_{45}MA$ was extracted with chloroform and roto-evaporated in order to obtain a dry white waxy solid. ET-743 and its clinical formulation Yondelis® (powder: 0.25 mg of trabectedin, 2 mg of potassium and 0.1 g of sucrose) were kindly provided by Dr. Carmen Cuevas, PharmaMar S.A. Colmenar Viejo (Madrid), Spain.

2.2. Synthesis of a PCL-based macromonomers

A PCL-based oligo-ester that bears a double bond was synthesized via the macromonomer method according to a procedure previously

reported in literature [27]. As reported in the step I of Fig. S1 (Supporting information, SI), the ring opening polymerization of CL was carried out in the presence of HEMA as initiator and stannous octanoate as co-catalyst. The CL to HEMA that corresponds to the subscript q in Fig. S1 (SI) was set equal to 5 while the HEMA to stannous octoate ratio was set equal to 1/200. Briefly, 11.84 g of CL and 11.84 mg of Na_2SO_4 were weighted in a septa-sealed flask and heated to 130 °C in a constant temperature oil bath under stirring. 2.7 g of HEMA were mixed with 42.02 mg of $Sn(Oct)_2$ in a different vial and injected into the pre-heated CL containing flask. The polymerization was left to proceed for 3 h. An aliquot was taken to evaluated the average number of CL units attached to HEMA (q) via near magnetic resonance (^{1}H NMR) according to a previously reported method [27] (q = 5.4).

2.3. Synthesis of the PEG-based hydrophilic block

The hydrophilic part of the block-copolymer was synthesized via the RAFT polymerization of $PEG_{45}MA$ in the presence of CPA as RAFT agent and ACVA as initiator according to a procedure previously reported [28] and as shown in the step II of Fig. S1 (SI). Briefly, the RAFT polymerization was carried out in ethanol with a CPA to ACVA molar ratio equal to 1/5 and a $PEG_{45}MA$ to CPA molar ratio equal to 5. 3.94 g of $PEG_{45}MA$, 110 mg of CPA and 15 mg of ACVA were dissolved in 20 ml of ethanol and poured in a septum sealed flask. The mixture was purged with nitrogen for 20 min and heated to 65 °C in a controlled temperature oil bath. After 24 h, 22.11 mg more of ACVA in 1 ml of ethanol were added to the mixture to re-start the polymerization. After another day, the polymer was precipitated in diethyl ether and dried under nitrogen. Number average molecular weight (*Mn*), dispersity (*Đ*) and conversion (*X*) were evaluated via GPC according to a previous procedure [29] (*Mn* = 11,935 g/mol, *Đ* = 1.04, *X* = 86.5%).

2.4. Synthesis of the amphiphilic block-copolymers

A library of amphiphilic block-copolymers was synthesized as reported in the step III of Fig. S1 (SI) via the RAFT polymerization of the PCL-based macromonomer previously obtained in the step I in the presence of the PEG-based hydrophilic block as macro-RAFT agent and ACVA as initiator. The PCL-based macromonomer (HEMA-CL_5) to $PEG_{45}MA$ molar ratio that corresponds to the subscript *p* in Fig. S1 (SI) was varied in order to obtain block-copolymers with different number of lipophilic brushes. The $5PEG_{45}MA$ to ACVA molar ratio was set constant and equal to 1/3. As an example, for the block-copolymer with *q* = 5 and *p* = 10, 0.469 g of $5PEG_{45}MA$, 0.32 g of HEMA-CL_5 and 4.3 mg of ACVA were dissolved in 4 ml of ethanol and poured in a 4 ml vial. The mixture was purged with nitrogen for 4 min and then was heated to 65 °C in a controlled temperature oil bath under stirring. After 24 h, the final material was precipitated several times in diethyl ether and dried under air. *Mn* and *Đ* were determined by GPC.

2.5. Synthesis of NPs

NPs were synthesized via the direct self-assembly of the block-copolymers into PBS. Briefly, different amounts of block-copolymer (7.5 mg, 15 mg, 30 mg, 60 mg) were dissolved in DMSO at different concentrations ($C_{P/D}$ = 27.5, 55, 110, 220 mg/ml) and aspired by a syringe with a needle pre-filled with 3 ml of PBS. The mixture was ejected and aspired three times. As a comparison, a second method of NP production that consists of the use of a T-mixer was carried out according to a procedure and a set-up previously published [16]. Briefly, the block-copolymer was dissolved in DMSO at a concentration of 27.5 mg/ml and injected with a syringe pump radially in the T-mixer at a flow rate of 2.7 ml/min, whereas PBS was injected countercurrent at a flow rate of 30 ml/min. All the NPs were produced three times and each of the resulting NP dispersions was analyzed via dynamic light scattering (DLS) to investigate quality, size (Dn) and polydispersity (PdI).

2.6. Characterization techniques

GPC analyses were performed with a Jasco (Series) apparatus. Samples were dissolved in THF at a concentration of 4 mg/ml and filtered through a 0.45 μm pore-size membrane. The separation was performed at a flow rate of 0.5 ml/min and at 35 °C with three Superchrom PLgel 5 μm columns (600 × 7.5 mm, measuring range 0.5–1000 kDa). *Mn* and *Đ* were determined from differential refractive data and were relative to poly(styrene) standards.^{1}H NMR analyses were performed in $CDCl_3$ on a Bruker Spectrometer (400 MHz). NP Dn and PdI measurements were obtained via DLS with a Zetasizer Nano (Malvern Instruments) and are relative to intensity. All the reported data are an average of three different measurements.

2.7. ET-743 loading and release

The loading of the ET-743 in the NPs was carried out during the self-assembly of the block-copolymer into PBS. 80 μg of ET-743 were mixed with DMSO and the block-copolymer with *q* = 5 and *p* = 10 at three ET-743 to block-copolymer ratios (ET/*P* = 19.3, 9.6, 4.8 μg/mg) and at $C_{P/D}$ = 220 mg/ml. Then the same syringe method described above was adopted for the synthesis of the NPs. 0.5 ml of the final latex (corresponding to the t0 of the subsequent release experiment) was used to evaluate the ET-743 loading. 2.5 ml of the final latex was injected in a 3.5 MWCO membrane cassette and a dialysis against 200 ml of PBS was performed. Aliquots of 0.1 ml of the latex were withdrawn after 1, 4, 6 and 24 h to investigate the ET-743 release. The experiment was repeated three times and PBS was changed frequently to assure sink conditions.

2.8. Pharmacokinetic study and antitumor activity

Procedures involving animals and their care were conducted in conformity with the following laws, regulations, and policies governing the care and use of laboratory animals: Italian Governing Law (D.lgs 26/2014; Authorization n.19/2008-A issued March 6, 2008 by Ministry of Health); Mario Negri Institutional Regulations and Policies providing internal authorization for persons conducting animal experiments (Quality Management System Certificate – UNI EN ISO 9001:2008 – Reg. N° 8576-A); the NIH Guide for the Care and Use of Laboratory Animals (2011 edition) and EU directives and guidelines (EEC Council Directive 2010/63/UE) and in line with Guidelines for the welfare and use of animals in cancer research. Animal experiments has been reviewed and approved by the IRFMN Animal Care and Use Committee (IACUC) that includes members “ad hoc” for ethical issues. Animals were housed in the Institute's Animal Care Facilities, which meet international standards; they are regularly checked by a certified veterinarian who is responsible for health monitoring, animal welfare supervision, experimental protocols and procedures revision. The new NP based formulation was firstly tested in C57BL6/J healthy mice (Charles River, Calco, Italy). The pharmacokinetic profile of the NPs loaded with ET-743 (ET-NPs) was compared to that of the clinical formulation of the drug (Yondelis®). Mice were treated i.v. at the dose of 0.15 mg/kg with the two formulations. Blood samples were collected in heparinized tubes from the retro-orbital plexus under isoflurane anesthesia, after treatment at the following time points: 5, 10, 30 min, 1, 3, 6 and 24 h. Then mice were sacrificed by cervical dislocation and liver, kidney, lung, heart and spleen removed and immediately frozen in dry-ice. To obtain plasma, blood samples were centrifuged at 4000 rpm for 10 min at 4 °C. All the collected samples were stored at −20 °C until analysis. The total concentration of ET-743 (ET-743 inside NPs plus ET-743 free) in the different biological matrices was determined by LC-MS/MS as previously described [30,31]. To determine the antitumor activity and tolerability of ET-NPs, tumor fragments of ML017myxoid liposarcoma

xenograft were engrafted subcutaneously on the flank of 7 weeks old female athymic nude mice (Envigo RMS, Udine, Italy). Tumor growth was monitored once a week by Vernier caliper and tumor volume calculated as follow: length × (width)^2 / 2. When tumor weight achieved about 350 mg, mice were randomized into the experimental groups. Mice were treated i.v. at 0.075 mg/kg and 0.15 mg/kg with the Yondelis®, ET-NPs, with empty NPs and saline as control. The treatment was repeated three times every week (q7dx3) for the antitumor activity evaluation. Toxicity was evaluated on the basis of body weight loss (BWL), clinical observation and mortality. Moreover, in a separate group of mice the serum levels of hepatic enzymes alanine aminotransferase (ALT) and aspartate aminotransferase (AST), and the bilirubin concentration (TBIL) were evaluated 48 h after the third dose in order to compare the hepatic toxicity of the ET-NPs and the Yondelis® formulations. In parallel to the antitumor activity study, the drug levels after both acute and chronic treatments were assessed in blood, tumors and livers of tumor bearing mice. Samples were collected at 1, 4, 24 and 48 h after acute treatment and 1 and 24 h after chronic treatment (q7dx3) and managed as reported above. Statistical analysis was performed with GraphPad Prism version 6.01 software (GraphPad software, Inc., La Jolla, CA, U.S.A.). Student's *t*-test was performed to compare drug content in the different biological matrices and hepatic enzyme serum levels. p-Value < 0.05 was considered significant.

2.9. Histopathological analysis

To evaluate the vascular and perivascular toxicity at the injection site, groups of at least five C57BL/6 mice were treated i.v. with, Yondelis® 0.15 mg/kg, ET-NPs 0.15 mg/kg or the correspondent controls (saline and empty NPs). One week after treatment, mice were sacrificed, tail removed and fixed in 10% buffered formalin for the histological analysis. Formalin fixed tails were decalcified in EDTA 10% acid free for 10 days and routinely processed for paraffin embedding. Samples were then sectioned at 4 µm thickness. Two transversal sections from proximal and distal region and one longitudinal section intermediate region of each tail were stained with hematoxylin and eosin and evaluated under a light microscope. The dermal inflammatory infiltrate, epidermal lesions (hyperplasia/dysplasia) and other lesions (dermo-epidermal detachment) were analyzed and scored for their severity and distribution according to the evaluation scheme reported in Table S1 (SI).

3. Results and discussion

3.1. NP synthesis and formulation optimization

PCL-based block-copolymers were synthesized via two subsequent RAFT polymerizations of a PEG-based methacrylate and of a PCL-based methacrylate, the latter one obtained via the ring opening polymerization of CL in the presence of HEMA as initiator. These block-copolymers are made up of hydrophilic part (PEG) and a biodegradable lipophilic one, so that they can self-assemble into NPs once nanoprecipitated in an aqueous phase. The main advantage of this system compared to the linear PCL-PEG block-copolymer developed so far [19] is that they have an additional degree of freedom that comes from their particular comb-like structure [32,33]. In fact, in addition to the length of the PCL chains, it is also possible to control the number of the chains via the adoption of a controlled radical polymerization, such as the RAFT polymerization [33–35]. This additional architectural complexity can be exploited to produce libraries of block-copolymers with different properties (e.g. biodegradation time). However, the need of devices, such as a T-mixer [16,32], are often required to increase the turbulence of the NP formation during the production step leading to a set up that cannot be easily translated directly into a hospital and/or at the bed of the patient. In addition, as long as the NPs are biodegradable, the obtained formulation needs to be immediately used or stored dry in order to assure a good shelf-life [17]. This, requires a lyophilization step that may lead to NP aggregation during the freezing step [18]. For this reason, in this work, a method that consists of the use of a simple syringe at the patient bed has been developed to eliminate the need of turbulence enhancer instruments; the lipophilic drug and the block-copolymer are dissolved in a small amount of DMSO and then aspired with a syringe pre-filled with the aqueous phase. The turbulence necessary for the correct formation of the NPs is here provided by some cycle of aspiration and ejection of the mixture through the needle of the syringe. In addition, a filtration through a 0.22 µm filter syringe is applied to eliminate possible precipitated or dispersed drug and to provide sterilization before injection. However, the approach requires the optimization of the block-copolymer, of the nanoprecipitation conditions in the NP formation and the correct choice of the block-copolymer concentration in DMSO ($C_{P/D}$). For these reasons, the additional degree of freedom of the brush-like structure is useful to develop a library of NP with different size and properties and to reduce the final concentration of the water-soluble organic solvent (C_{DMSO}). In order to demonstrate this approach, a series of PCL-based block-copolymers was synthesized keeping the number of hydrophilic chains equal to 5 and varying the number (p from 5 to 50) of the lipophilic chains with 5 CL units ($q = 5.4$). As shown in Fig. 1a, all the block-copolymers synthesized exhibit a very low $Đ$ and the Mn is a linear function of p, as expected from a RAFT polymerization [29]. In a similar way, the NP Dn synthesized via the syringe method and the T-mixer from the block-copolymers at $C_{DMSO} = 8.3\%$ and at $C_{P/D} = 27.5$ mg/ml are a linear function of p (Fig. 1b). However, as long as the turbulence conditions in a mixing device are more favorable compared to the ones in a needle of

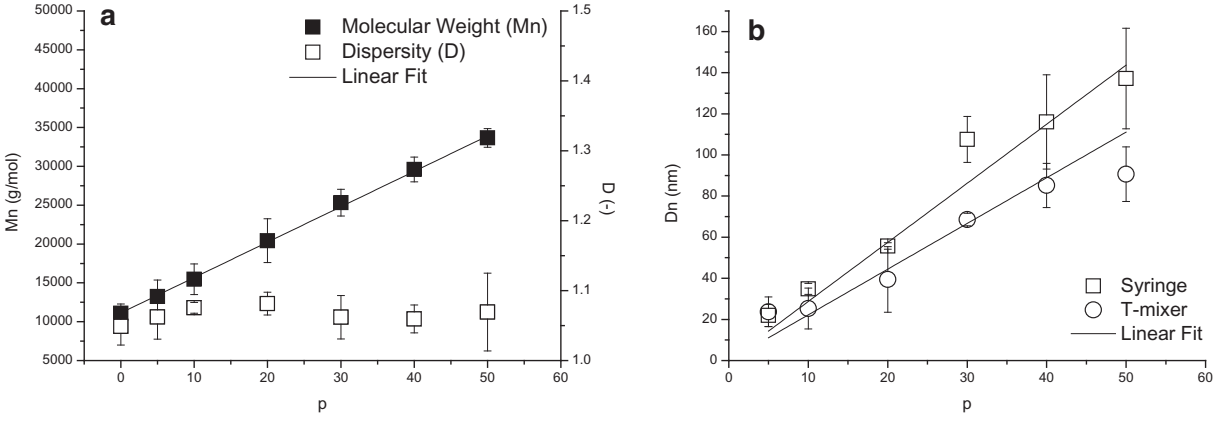

Fig. 1. a) *Mn* and *Đ* of the block-copolymer synthesized as a function of the number of lipophilic chains (p); b) NP *Dn* synthesized with the T-mixer and the syringe method from the block-copolymers at $C_{P/D} = 27.5$ mg/ml and $C_{DMSO} = 8.3$ vol.%.

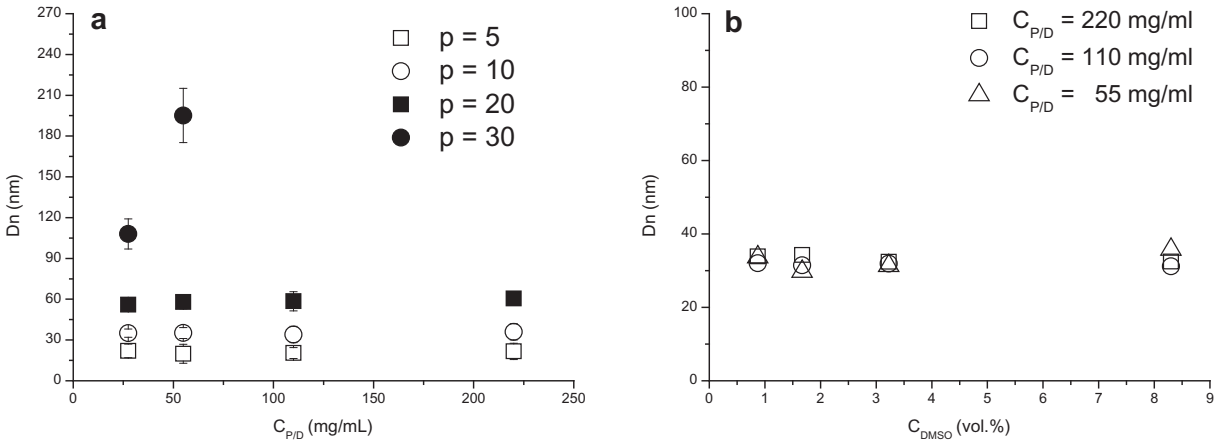

Fig. 2. a) NP Dn as a function of $C_{P/D}$ at different number of lipophilic chains (p) b) NP Dn as a function of the C_{DMSO} at different $C_{P/D}$ for the block-copolymer with $q = 5$ and $p = 10$.

Table 1
Three NP formulations with ET-743 at different C_{DMSO} and ET/P ratios.

Formulation	C_{DMSO}	ET/P	$C_{P/D}$	Dn	PdI	Loading efficiency
#	vol%	μg/mg	mg/ml	nm	–	%
1	0.75	19.3	220	34	0.190	97
2	1.49	9.6	220	34	0.166	99
3	2.94	4.8	220	32	0.141	98

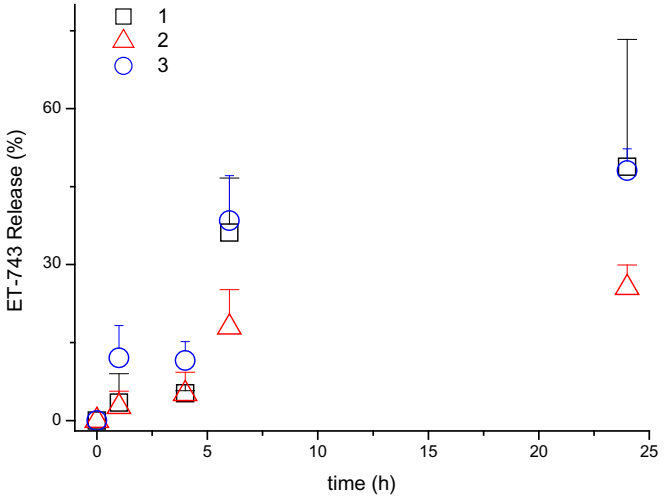

Fig. 3. ET-743 Release at different C_{DMSO} and ET/*P* values with a $C_{P/D}$ equal to 220 mg/ml.

a syringe, the NP sizes obtained with this latter one are bigger and the difference between the two methods increases as the *p* increases, even if the PdIs are not significantly different (PdI varies from 0.114 to 0.260 for both the methods, as evident from Table S2, SI).

This suggests that the block-copolymer is not able to correctly rearrange when its lipophilicity becomes too high. In fact, it is well known that a fast mixing between the organic and the aqueous phase leads to smaller NPs because in these conditions the insertion and exchange of the unimers (single amphiphilic chains) is favored and the overall improvement depends on the length and the nature of the lipophilic part of the block-copolymer [15]. However, surprisingly, the turbulence conditions do not influence the linear trend of the NP size with *p*. In fact, this behavior is a general phenomenon linked to the geometrical disposition of the block-copolymers that forms the NPs when the lipophilic part of the block-copolymer is segregated inside the NP core and the hydrophilic chains are confined on the NP surface as summarized by eq. (1) [29]:

$$Dn = \frac{6 \cdot p \cdot MW_{HEMA-CL5}}{N_{Avo} \cdot A_{Cov} \cdot \rho_{b,lipo}} = \frac{6 \cdot MW_{b,lipo}}{N_{Avo} \cdot A_{Cov} \cdot \rho_{b,lipo}} \quad (1)$$

where $MW_{HEMA-CL5}$ is the molecular weight of the lipophilic monomer, ρ_{b_lipo} and MW_{b_lipo} the density and molecular weight of the lipophilic part of the block-copolymer, respectively, N_{avo} the Avogadro number, and A_{Cov} the surface area that the hydrophilic part of the block-copolymer can cover. It may be possible that the turbulence conditions of the production step may have an important impact on the hypothesis that the hydrophilic chains are completely located on the NP surface. If they have not enough time to rearrange, some of them may be buried inside the core [15], affecting their ability to stabilize the NP and thus resulting in a lower A_{Cov}, as visible in the higher slope of the NP Dn obtained with the syringe method compared to the T-mixer in Fig. 1b. It is worth mentioning that, as long as the NP PdI are high due to the difficulties in the chain rearrangement during a common nanoprecipitation step independently from the method adopted, a perfectly homogenous and ordered configuration of the block-copolymers in all the NPs is in any case very unlikely. In fact, on the contrary of micelles produced via surfactants, nanoprecipitation generates kinetically frozen NPs that are not in a thermodynamic equilibrium due to diffusion limitations [36]. Another important parameter of the nanoprecipitation step that affects the quality of the obtained NPs is the concentration of the block-copolymer in DMSO ($C_{P/D}$). This must be high in order to reduce the organic solvent necessary (C_{DMSO}) for the formation of the NPs and to avoid solvent related side effects, even if DMSO is generally considered safe at high doses [37–39] and poorly cytotoxic at concentration lower than 10 vol% [40,41], and that a stem-cell suspension with 10 vol% DMSO have been already approved for i.v. infusion in Canada and New Zealand in 2012 (Prochymal, Osiris Therapeutics) [42]. For example, it is possible to obtain well-defined NPs via the syringe method with no changes in their sizes across a large interval of $C_{P/D}$ (Fig. 2a) for the block-copolymers with $q = 5$ and $p = 5$, 10 and 20. This indicates that the mixing time for these species is lower than the characteristic time of the aggregation process and then that the NP size is independent of polymer concentration in the organic phase [43]. However, with *q* higher than 20, NP Dn increases as the $C_{P/D}$ increases until it is no longer possible to obtain good quality NPs. It is also worth mentioning that the materials not affected by the increase in the $C_{P/D}$ are also the ones that present the lower variation in Dn when produced via T-mixer and syringe method (Fig. 1b) indicating that they are in general less affected by the turbulence conditions of the production step due to their overall lower lipophilicity. Among them, the one with $q = 5$ and $p = 10$ has also been used to test the impact of the C_{DMSO} on the NP formation at all the evaluated $C_{P/D}$ (Fig. 2b). For this block-

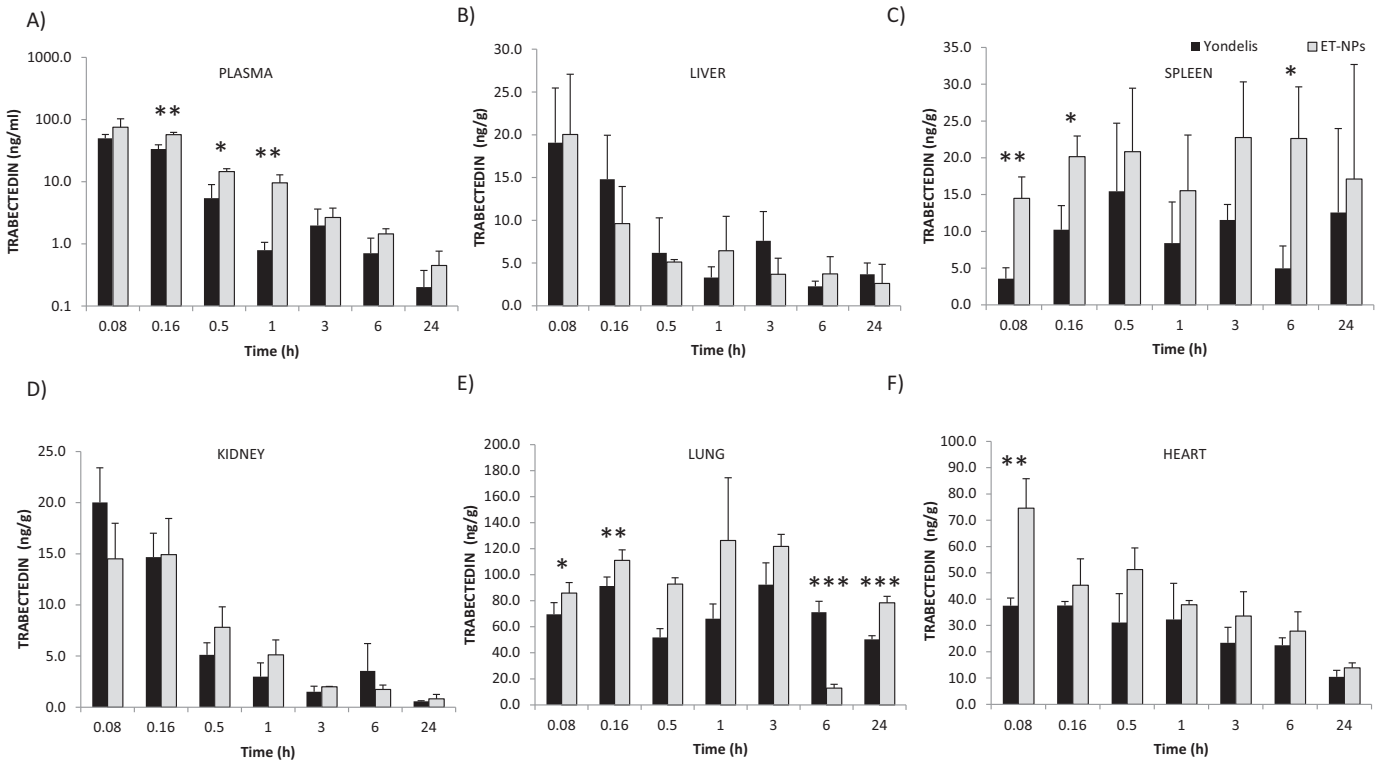

Fig. 4. Comparison of the ET-743 plasma levels (A) and distribution in liver (B), spleen (C), kidney (D), lung (E) and heart (F) of healthy *C57BL6/J* mice after administration of a single treatment of Yondelis® or ET-NPs (0.15 mg/kg i.v.) (mean ± s.d. *Student *t*-test p-value < 0.05; **Student *t*-test p-value < 0.01; ***Student *t*-test p-value < 0.001).

Table 2
Main pharmacokinetic parameters determined for ET-743 (0.15 mg/kg i.v.)

Formulation	Matrix	C_{max} (Co)	T_{max}	$AUC_{0\text{-}last}$	AUC_{inf}	HL	Cl_p	V_d
		ng/ml or /g	h	ng/ml or /g*h	ng/ml or /g*h	h	L/h/kg	L/kg
Yondelis®	Plasma	49.8 (73.7)	–	31.4	33.5	7.3	4.5	46.9
ET-NPs		73.7 (99.0)	–	65.8	71.6	8.9	2.1	26.9
Yondelis®	Liver	19.1	0.08	87.5	–	–	–	–
ET-NPs		20.0	0.08	85.9	–	–	–	–
Yondelis®	Spleen	15.5	0.5	213.5	–	–	–	–
ET-NPs		22.8	3.0	482.0	–	–	–	–
Yondelis®	Kidney	20.0	0.08	56.7	–	–	–	–
ET-NPs		14.9	0.16	44.3	–	–	–	–
Yondelis®	Lung	92.4	3.0	1561.7	–	–	–	–
ET-NPs		126.3	1.0	1372.1	–	–	–	–
Yondelis®	Heart	37.6	0.16	452.4	–	–	–	–
ET-NPs		74.6	0.08	585.5	–	–	–	–

copolymer, the syringe method is a very robust and reproducible method to produce NPs as long as it does not show any significant change in Dn across all the conditions tested. As a result, this block-copolymer has been chosen as candidate for the drug delivery of ET-743.

3.2. ET-743 loading and release

$C_{P/D}$ and C_{DMSO} are important parameters in a nanoprecipitation method that has the final goal of allowing the end-user to formulate the drug directly at the bed of the patient without intermediate purification steps. In fact, these two parameters do not only affect the quality of the produced NPs and the overall toxicity of the formulation, but they are also responsible for the loading capacity of the carrier and for the ability to retain the drug inside. However, the amount of drug necessary to reach an adequate therapeutic level is another important factor that needs to be considered in the design of the final NP formulation. In order to study the influence of these parameters, three formulations were produced by varying the amount of C_{DMSO} in order to obtain different ET-743 to block-copolymer (ET/P) ratios. As visible in Table 1, NP Dn and PdI are not affected by the amount of ET-743 and the loading efficacy with the syringe method is very high (97–99%). This latter result indicates that only a small drug amount precipitates and/or is eliminated by filtration with the 0.22 μm syringe filter.

The partition of the ET-743 in the lipophilic core of the NPs and in the aqueous medium depends on the lipophilicity of the drug itself and, of course, on C_{DMSO}. As long as ET-743 is freely soluble in DMSO, the higher the C_{DMSO}, the higher the amount of drug in the aqueous phase. On the contrary, a small amount of DMSO results in a high ET/P value (Table 1), a high amount of drug inside the NP and thus a higher concentration gradient across the two phases. These opposite phenomena explain why the formulation with the highest C_{DMSO} (formulation 3 in Table 1) and the one with the highest ET/*P* value (formulation 1 in Table 1) show a faster release of the drug in PBS compared to the one with intermediate values (formulation 2), as visible in Fig. 3.

For this reason, even though all the formulations show a low release after 4 h indicating the ability of the NPs to retain the therapeutic inside the core for a time sufficient for the i.v. administration to the patient, the one with the lowest release at 24 h has been chosen for the subsequent in vivo studies.

3.3. Pharmacokinetic study

The pharmacokinetic of this NP-based ET-743 formulation (formulation 2 in Table 1 and hereafter referred to as ET-NPs) in comparison with the commercially available ET-743 formulation (Yondelis®) has been studied determining total levels of ET-743 (ET-743 inside NPs

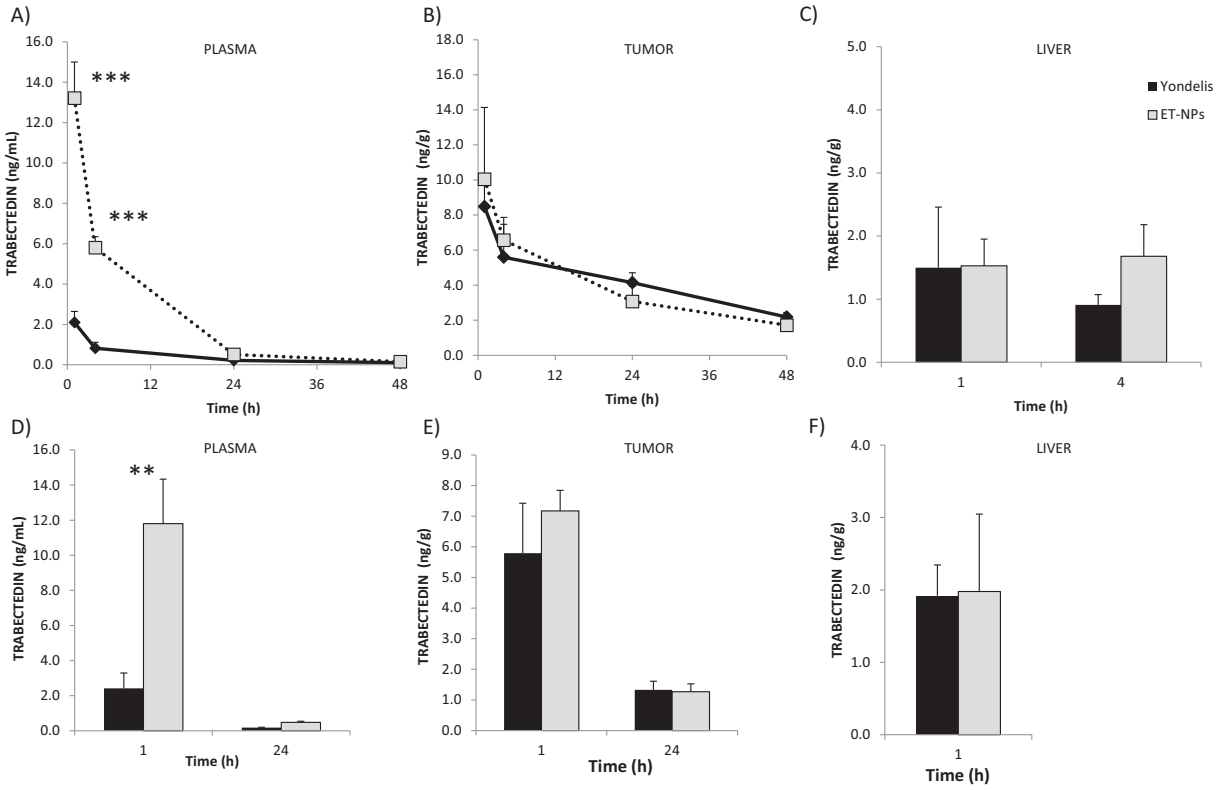

Fig. 5. Comparison of the ET-743 distribution in plasma (A), tumor (B) and liver (C) of ML017 bearing mice after administration of an acute dose of Yondelis® or ET-NPs (0.15 mg/kg i.v.) and plasma (D), tumor (E) and liver (F) after chronic treatment *q7dx3* of Yondelis® or ET-NPs (0.15 mg/kg i.v.) (mean ± s.d. *Student *t*-test p-value < 0.05; **Student *t*-test p-value < 0.01; ***Student *t*-test p-value < 0.001).

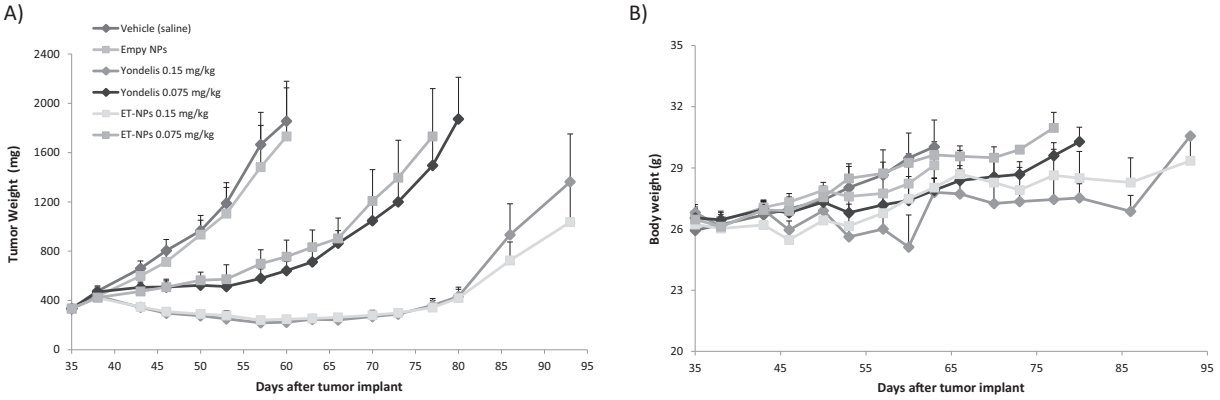

Fig. 6. a) Antitumor activity of Yondelis® and ET-NPs against ML017cancer model at two different doses. b) Animal body weight during treatment and subsequently (B). Results represent the mean ± SEM (n = 10).

plus ET-743 free) in plasma, liver, kidney, heart, lung and spleen of healthy mice. The specimens were collected at different time points after drug injection. As shown in Fig. 4, the distribution of Yondelis® and ET-NPs was comparable only in liver and kidney. In plasma, the administration of ET-NPs leads to higher circulating concentration compared to Yondelis® especially at the early time points with a maximum difference 1 h after treatment (Yondelis® = 0.79 ± 0.26 ng/ml; ET-NPs = 9.56 ± 3.31 ng/ml; *t*-test p-value = 0.010). This can be due to the drug initial retention into the nanoparticles causing a slower tissue distribution.

The main PK parameters are summarized in Table 2. Plasma C_{max} (Co) of ET-743 corresponds to 49.8 ng/ml (73.7) after the Yondelis® and 73.7 (99.0) ng/ml after ET-NPs. This difference in concentration was particularly evident at 1 h and is maintained up to 24 h. Consequently, a two time increase of AUC can be highlighted in plasma and spleen of animals treated with ET-NPs in comparison with those treated with Yondelis®. After the distribution phase, the drug is eliminated from plasma with the same half-life (about 7-8 h). The values of Cl_p (4.5 vs 2.1 L/h/kg for Yondelis® and ET-NPs) indicate a slower elimination of ET-NPs from the plasma compartment. The difference in plasma AUC is evident but not reflected by a substantial variation in the AUC of lung and heart even if higher C_{max} levels are reached with ET-NPs than with Yondelis®.

A further confirmation of the pharmacokinetic behavior outlined above was found by examining the amount of ET-743 recovered in the different tissue in tumor bearing mice after acute or chronic administration of the two formulations. As shown in Fig. 5, there is no significant difference in the ET-743 concentration measured in tumor and liver at different time points after both single and repeated treatment (q7dx3) with Yondelis® or ET-NPs at dose of 0.15 mg/kg. As highlighted

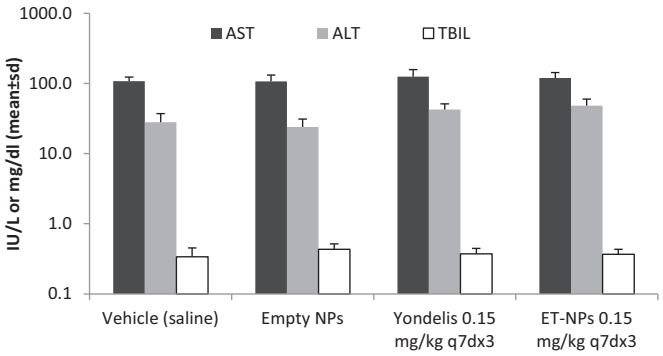

Fig. 7. Evaluation of serum hepatic enzymes activity (AST and ALT) and bilirubin concentration (TBIL) after treatment with Yondelis®, ET-NPs, empty NPs and vehicle.

in the previous experiment, the difference in the plasma drug concentration is confirmed in both the treatment schedules. We do not know why the different plasma concentration is not translated in a different tumor concentration of ET-743. We can speculate that at least at early time points part of the drug plasma concentration is still bound to the nanoparticles and thus not available for the tissue distribution. This explanation is in keeping with the finding that in spleen, an organ known to entrap nanoparticles, the concentration of ET-743 is higher after administration of ET-NPs than after Yondelis®.

Taken together, these results suggest that not all of the lipophilic drug loaded on the NPs is released immediately after the injection leading to a higher concentration in plasma (Fig. 4A) and in the spleen (Fig. 4C), an organ where nano-metric objects are often cleared by phagocytic uptake [44]. On the contrary, the amount of ET-743 recovered into the liver (Figs. 4C and 5C, F), another organ responsible for the elimination of the NPs [44,45], is the same for both the formulations, suggesting that the metabolism of trabectedin is not affected by the formulation in NPs. In addition, the NPs are big enough to not be filtered by the kidneys [13], as suggested by the same ET-743 concentration found in this organ for both Yondelis® and ET-NPs (Fig. 4D).

3.4. Safety and antitumor activity

ET-NPs and Yondelis® antitumor activity has been studied at two different doses (0.15 mg/kg and 0.075 mg/kg). At the optimal dose of 0.15 mg/kg, all treatments were very active with a best T/C of 10.8% and 11.2% on day 63 for Yondelis® and ET-NPs, respectively. Comparable T/C values of 31.1% and 36.4% for Yondelis® and ET-NPs, respectively, were observed even at the lower dose of ET-743, thus confirming the superimposable antitumor efficacy of the two formulations, shown in Fig. 6a. It is worth noting that no body weight loss was observed, and the evolution of the body weight is very similar to the

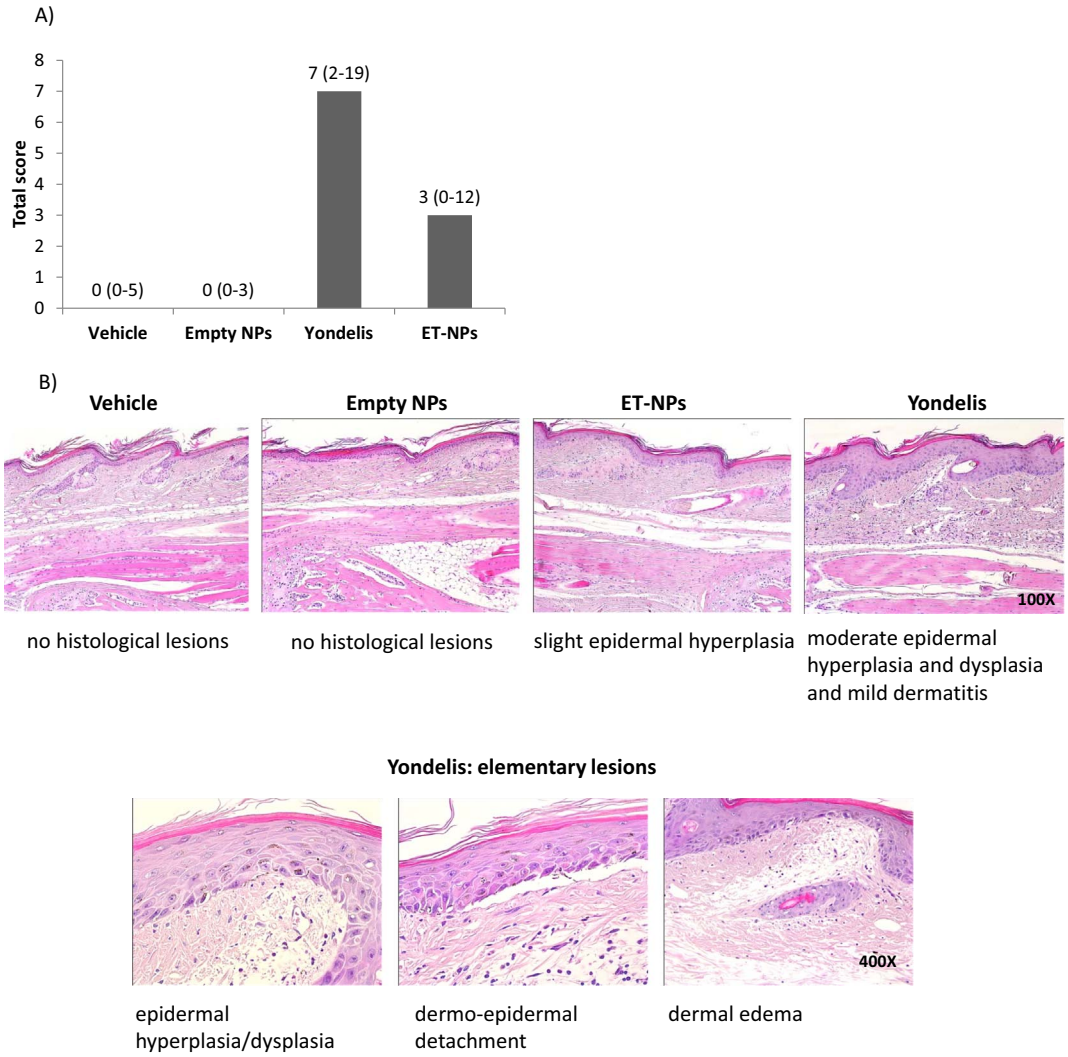

Fig. 8. Panel A: Total score (median and range) calculated by summing up the scores obtained by each mouse for all the histopathological features evaluated. Panel B: H&E staining of the tails injected with saline, empty NPs, ET-NPs and Yondelis®.

control for all the treatment groups with an overall increasing trend, as shown in Fig. 6b. These data suggest that the toxicity of the produced formulation is comparable to Yondelis® and is not remarkable. No statistical differences were found in the body weight of animals receiving empty NPs, suggesting that they do not cause detectable toxicity in these conditions.

For a more in-depth analysis of the safety profile, the evaluation of serum activity of hepatic enzymes and of the serum total bilirubin concentration was carried out; the results indicate that there is no increased hepatic toxicity administering ET-743 formulated in NPs as compared with Yondelis® (Fig. 7).

3.5. Histopathological analysis

Trabectedin is a potent anticancer therapeutic that cause phlebitis at the site of injection. This local vascular toxicity makes it mandatory to administer the drug by a central venous catheter placed in a large vein. This method of administration generally prevents acute vascular toxicity even though erythema along the blood vessels and residual sclerotic phlebitis have also been reported in this case [26]. In addition, the use of venous catheters do not only reduce the patient compliance to the treatment, but it also increases the risks and occurrence of infections and thromboses, as reported by Roylance et al. [46] in 15% and 5% of the cases, respectively. For this reason, local adverse effects of Yondelis® and ET-NPs injected into tail vein were assessed after treatment. The histopathological features analyzed were dermal edema and inflammatory infiltrate, epidermal lesions (hyperplasia/dysplasia) and dermo-epidermal detachment and were evaluated basing on the severity and distribution score described in Table S1 (SI). As shown in Fig. 8 panel A, Yondelis® presents very high scores in the severity and distribution of all the lesions considered for an overall median score of 7 in good agreement with the toxicity of the Yondelis® observed in patients. On the contrary, ET-NPs presents a significantly reduced median score of 3, while the empty NPs have a score equal to 0. Detailed score values for each pathological feature are reported in Table S3 in SI. A similar result can be seen in the H&E staining of the tails of control mice (treated with saline solution or empty NPs) in Fig. 8 panel B that does not show any kind of lesion with tissues showing normal histological appearance. The tails of mice treated with Yondelis® exhibits severe epidermal lesions with area characterized by lysis of the basal layer resulting in complete epidermal detachment. There are moderate hyperplasia and dysplasia of the epidermal cells. In dermis, inflammatory cells and edema are present. In contrast, tails of mice treated with ET-NPs do not display epidermal detachment and few, minor findings of epidermal hyperplasia/dysplasia, and dermal inflammatory cells or edema.

In summary, the NPs are able to retain the drug inside the core for a time long enough to reduce the adverse local vascular effect of Yondelis®, permitting the i.v. administration of ET-743 in a peripheral vein, with obvious medical advantages and reduced cost.

4. Conclusions

In conclusion, a nanoprecipitation procedure to formulate lipophilic anticancer therapeutics into NPs directly at the bed of the patient has been developed. This method consists of the use of a syringe with a needle, a small amount of organic solvent and of an amphiphilic block-copolymer. The effective synthesis of NPs has been made possible due to the optimization of the block-copolymer via a combination of RAFT and ROP polymerization and the fine tuning of the main parameters of the final formulation. The NPs has been used to formulate trabectedin, an anticancer therapeutic known for its local adverse effect, with only 1.5 vol.% of DMSO in the final mixture. The pharmacokinetic behavior, antitumor activity and toxicity of this NP-based formulation have been compared to those of Yondelis®. NPs have shown the ability to retain the drug in circulation for a time long enough to considerably reduce the local vascular toxic effects, as proven by the histopathological analysis performed, and without affecting the drug ability to reduce the tumor growth. This solution paves the way to a classic i.v. administration in a peripheral vein of ET-743, reducing both the risk and occurrence of infections and thromboses caused by venous catheters as well as the health care costs associated with the treatment. In addition, the shift of the NP preparation step from a specialist to the final user eliminates the need for the purifications and post-processing steps necessary to assure a good shelf-life of the product. In this way, a ET-743 formulation that is less toxic than the commercially available Yondelis® can be produced at a competitive price, also taking into account that this expensive drug is not lost in any of the NP production steps adopted here, in sharp contrast with the common procedures of drug loading and purification generally adopted.

Conflict of interest

Umberto Capasso Palmiero, Massimo Morbidelli, Maurizio D'Incalci and Davide Moscatelli filed a patent application regarding this technological platform.

Acknowledgements

We acknowledge support from AIRC (10016) Special Program Molecular Clinical Oncology “5 per mille”.

Appendix A. Supplementary data

Supplementary data to this article can be found online at https://doi.org/10.1016/j.jconrel.2018.03.005.

References

[1] R.H. Prabhu, V.B. Patravale, M.D. Joshi, Polymeric nanoparticles for targeted treatment in oncology: current insights, Int. J. Nanomedicine 10 (2015) 1001.
[2] I. Brigger, C. Dubernet, P. Couvreur, Nanoparticles in cancer therapy and diagnosis, Adv. Drug Deliv. Rev. 64 (2012) 24–36.
[3] H. Maeda, J. Wu, T. Sawa, Y. Matsumura, K. Hori, Tumor vascular permeability and the EPR effect in macromolecular therapeutics: a review, J. Control. Release 65 (2000) 271–284.
[4] H. Maeda, Toward a full understanding of the EPR effect in primary and metastatic tumors as well as issues related to its heterogeneity, Adv. Drug Deliv. Rev. 91 (2015) 3–6.
[5] S. Wilhelm, A.J. Tavares, Q. Dai, S. Ohta, J. Audet, H.F. Dvorak, W.C. Chan, Analysis of nanoparticle delivery to tumours, Nat. Rev. Mater. 1 (2016) 16014.
[6] U. Prabhakar, H. Maeda, R.K. Jain, E.M. Sevick-Muraca, W. Zamboni, O.C. Farokhzad, S.T. Barry, A. Gabizon, P. Grodzinski, D.C. Blakey, Challenges and key considerations of the enhanced permeability and retention effect for nanomedicine drug delivery in oncology, Cancer Res. 73 (2013) 2412–2417.
[7] A. Bhatt, A. Ranade, 578P A retrospective observational study of efficacy and safety of Genexol-PM, a novel Cremophor-free, polymeric micelle formulation of paclitaxel, in patients with solid tumours, Ann. Oncol. 27 (2016).
[8] E. Miele, G.P. Spinelli, E. Miele, F. Tomao, S. Tomao, Albumin-bound formulation of paclitaxel (Abraxane® ABI-007) in the treatment of breast cancer, Int. J. Nanomedicine 4 (2009) 99.
[9] D.B. Resnik, S.S. Tinkle, Ethics in Nanomedicine, (2007).
[10] H. Ragelle, F. Danhier, V. Préat, R. Langer, D.G. Anderson, Nanoparticle-based drug delivery systems: a commercial and regulatory outlook as the field matures, Expert Opin. Drug Deliv. 14 (2017) 851–864.
[11] A. Wicki, D. Witzigmann, V. Balasubramanian, J. Huwyler, Nanomedicine in cancer therapy: challenges, opportunities, and clinical applications, J. Control. Release 200 (2015) 138–157.
[12] J.I. Hare, T. Lammers, M.B. Ashford, S. Puri, G. Storm, S.T. Barry, Challenges and strategies in anti-cancer nanomedicine development: an industry perspective, Adv. Drug Deliv. Rev. 108 (2017) 25–38.
[13] D. Moscatelli, M. Sponchioni, 12 - Bioresorbable polymer nanoparticles in the medical and pharmaceutical fields: A promising field, Bioresorbable Polymers for Biomedical Applications, Woodhead Publishing, 2017, pp. 265–283.
[14] S. Schubert, J.T. Delaney Jr, U.S. Schubert, Nanoprecipitation and nanoformulation of polymers: from history to powerful possibilities beyond poly (lactic acid), Soft Matter 7 (2011) 1581–1588.
[15] E. Lepeltier, C. Bourgaux, P. Couvreur, Nanoprecipitation and the “ouzo effect”: application to drug delivery devices, Adv. Drug Deliv. Rev. 71 (2014) 86–97.
[16] M. Sponchioni, U.C. Palmiero, D. Moscatelli, HPMA-PEG surfmers and their use in stabilizing fully biodegradable polymer nanoparticles, Macromol. Chem. Phys.,

1700380-n/a.
[17] W. Abdelwahed, G. Degobert, S. Stainmesse, H. Fessi, Freeze-drying of nanoparticles: formulation, process and storage considerations, Adv. Drug Deliv. Rev. 58 (2006) 1688–1713.
[18] M.K. Lee, M.Y. Kim, S. Kim, J. Lee, Cryoprotectants for freeze drying of drug nanosuspensions: effect of freezing rate, J. Pharm. Sci. 98 (2009) 4808–4817.
[19] E.A. Rainbolt, K.E. Washington, M.C. Biewer, M.C. Stefan, Recent developments in micellar drug carriers featuring substituted poly (ε-caprolactone) s, Polym. Chem. 6 (2015) 2369–2381.
[20] G. Valoti, M.I. Nicoletti, A. Pellegrino, J. Jimeno, H. Hendriks, M. D'Incalci, G. Faircloth, R. Giavazzi, Ecteinascidin-743, a new marine natural product with potent antitumor activity on human ovarian carcinoma xenografts, Clin. Cancer Res. 4 (1998) 1977–1983.
[21] M. D'Incalci, C.M. Galmarini, A review of trabectedin (ET-743): a unique mechanism of action, Mol. Cancer Ther. 9 (2010) 2157–2163.
[22] A.K. Larsen, C.M. Galmarini, M. D'Incalci, Unique features of trabectedin mechanism of action, Cancer Chemother. Pharmacol. 77 (2016) 663–671.
[23] M. Minuzzo, S. Marchini, M. Broggini, G. Faircloth, M. D'Incalci, R. Mantovani, Interference of transcriptional activation by the antineoplastic drug ecteinascidin-743, Proc. Natl. Acad. Sci. 97 (2000) 6780–6784.
[24] G. Germano, R. Frapolli, C. Belgiovine, A. Anselmo, S. Pesce, M. Liguori, E. Erba, S. Uboldi, M. Zucchetti, F. Pasqualini, Role of macrophage targeting in the antitumor activity of trabectedin, Cancer Cell 23 (2013) 249–262.
[25] P. Allavena, G. Germano, C. Belgiovine, M. D'Incalci, A. Mantovani, Trabectedin: a drug from the sea that strikes tumor-associated macrophages, Oncoimmunology 2 (2013) e24614.
[26] C. Sessa, F. De Braud, A. Perotti, J. Bauer, G. Curigliano, C. Noberasco, F. Zanaboni, L. Gianni, S. Marsoni, J. Jimeno, Trabectedin for women with ovarian carcinoma after treatment with platinum and taxanes fails, J. Clin. Oncol. 23 (2005) 1867–1874.
[27] R. Ferrari, Y. Yu, M. Morbidelli, R.A. Hutchinson, D. Moscatelli, ε-Caprolactone-based macromonomers suitable for biodegradable nanoparticles synthesis through free radical polymerization, Macromolecules 44 (2011) 9205–9212.
[28] U.C. Palmiero, A. Agostini, E. Lattuada, S. Gatti, J. Singh, C.T. Canova, S. Buzzaccaro, D. Moscatelli, Use of RAFT macro-surfmers for the synthesis of transparent aqueous colloids with tunable interactions, Soft Matter 13 (37) (2017) 6439–6449.
[29] U.C. Palmiero, A. Agostini, S. Gatti, M. Sponchioni, V. Valenti, L. Brunel, D. Moscatelli, Raft macro-surfmers and their use in the ab initio raft emulsion polymerization to decouple nanoparticle size and polymer molecular weight, Macromolecules 49 (2016) 8387–8396.
[30] L. Ceriani, M. Ferrari, M. Zangarini, S.A. Licandro, E. Bello, R. Frapolli, F. Falcetta, M. D'Incalci, R. Libener, F. Grosso, HPLC–MS/MS Method to Measure Trabectedin in Tumors: Preliminary PK Study in a Mesothelioma Xenograft Model, (2015).
[31] M. Zangarini, L. Ceriani, F. Sala, E. Marangon, R. Bagnati, M. D'Incalci, F. Grosso, M. Zucchetti, Quantification of trabectedin in human plasma: validation of a high-performance liquid chromatography–mass spectrometry method and its application in a clinical pharmacokinetic study, J. Pharm. Biomed. Anal. 95 (2014) 107–112.
[32] C. Colombo, S. Gatti, R. Ferrari, T. Casalini, D. Cuccato, L. Morosi, M. Zucchetti, D. Moscatelli, Self-assembling amphiphilic PEGylated block copolymers obtained through RAFT polymerization for drug-delivery applications, J. Appl. Polym. Sci. 133 (2016).
[33] M. Sponchioni, R. Ferrari, L. Morosi, D. Moscatelli, Influence of the polymer structure over self-assembly and thermo-responsive properties: the case of PEG-b-PCL grafted copolymers via a combination of RAFT and ROP, J. Polym. Sci. A Polym. Chem. 54 (2016) 2919–2931.
[34] J.L. Zhu, X.Z. Zhang, H. Cheng, Y.Y. Li, S.X. Cheng, R.X. Zhuo, Synthesis and characterization of well-defined, amphiphilic poly (N-isopropylacrylamide)-b-[2-hydroxyethyl methacrylate-poly (ε-caprolactone)] n graft copolymers by RAFT polymerization and macromonomer method, J. Polym. Sci. A Polym. Chem. 45 (2007) 5354–5364.
[35] J.-L. Zhu, H. Cheng, Y. Jin, S.-X. Cheng, X.-Z. Zhang, R.-X. Zhuo, Novel polycationic micelles for drug delivery and gene transfer, J. Mater. Chem. 18 (2008) 4433–4441.
[36] T. Nicolai, O. Colombani, C. Chassenieux, Dynamic polymeric micelles versus frozen nanoparticles formed by block copolymers, Soft Matter 6 (2010) 3111–3118.
[37] E.E. Vogin, S. Carson, G. Cannon, C.R. Linegar, L.F. Rubin, Chronic toxicity of DMSO in primates, Toxicol. Appl. Pharmacol. 16 (1970) 606–612.
[38] E. Fishman, L. Jenkins, R. Coon, R. Jones, Effects of acute and repeated inhalation of dimethyl sulfoxide in rats, Toxicol. Appl. Pharmacol. 15 (1969) 74–82.
[39] B.X. Hoang, D.M. Tran, H.Q. Tran, P.T. Nguyen, T.D. Pham, H.V. Dang, T.V. Ha, H.D. Tran, C. Hoang, K.N. Luong, Dimethyl sulfoxide and sodium bicarbonate in the treatment of refractory cancer pain, J. Pain Palliat. Care Pharmacother. 25 (2011) 19–24.
[40] J. Hebling, L. Bianchi, F. Basso, D. Scheffel, D. Soares, M. Carrilho, D.H. Pashley, L. Tjäderhane, C. de Souza Costa, Cytotoxicity of dimethyl sulfoxide (DMSO) in direct contact with odontoblast-like cells, Dent. Mater. 31 (2015) 399–405.
[41] J. GruberAllickson, B. Lenes, J. Bash, S. Smith, Cytotoxicity of DMSO to hematopoietic progenitor cells, in: transfusion, Am. Assoc. Blood Banks 8101 (20814–2749) (1997) S324 Glenbrook RD, Bethesda, MD.
[42] A.S.M.R. Strub, Advances in the Regulated Pharmaceutical Use of Dimethyl Sulfoxide USP, Ph. Eur (2016).
[43] B.K. Johnson, R.K. Prud'homme, Mechanism for rapid self-assembly of block copolymer nanoparticles, Phys. Rev. Lett. 91 (2003) 118302.
[44] F. Alexis, E. Pridgen, L.K. Molnar, O.C. Farokhzad, Factors affecting the clearance and biodistribution of polymeric nanoparticles, Mol. Pharm. 5 (2008) 505.
[45] M. Arruebo, R. Fernández-Pacheco, M.R. Ibarra, J. Santamaría, Magnetic nanoparticles for drug delivery, Nano Today 2 (2007) 22–32.
[46] R. Roylance, B. Seddon, A. McTiernan, K. Sykes, S. Daniels, J. Whelan, Experience of the use of trabectedin (ET-743, Yondelis™) in 21 patients with pre-treated advanced sarcoma from a single centre, Clin. Oncol. 19 (2007) 572–576.